Stripe antiferromagnetic ground state of ideal triangular lattice $KErSe_2$

– –

I. INTRODUCTION

These authors contributed equally

– –

II. MATERIALS AND METHODS

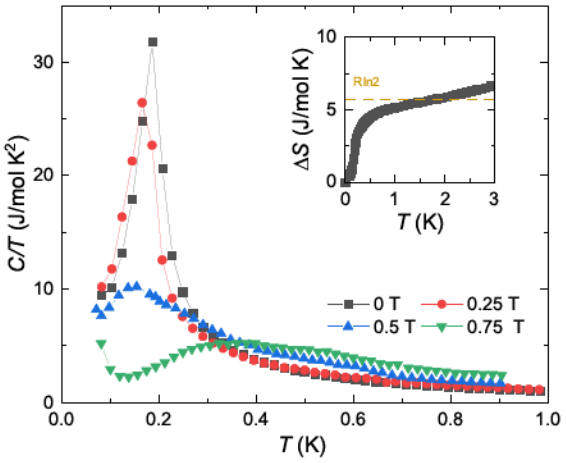

FIG. 1. Temperature dependence of heat capacity from 1 K to 0.08 K under different magnetic field. Inset: Temperature dependence of entropy at 0 T.

III. RESULTS AND DISCUSSION

A. Heat Capacity

Fig. 1 shows the temperature dependence of heat capacity of $KErSe_2$ from 1 K to 0.08 K. Above 0.4 K, no long-range order is found in the previous report up to 9 T [40]. At zero field, an apparent λ shape anomaly was found at ∼0.2 K with a tail up to ∼0.4 K, revealing a second order phase transition in $KErSe_2$. The inset of Fig. 1 presents the temperature dependent of entropy at 0 T. The released entropy is only close to 3 J/mol K at the transition and increases to the expected value Rln2 for Kramer doublets at ∼2 K. This found, similar to the previously reported Ce/Yb [33, 37], indicates the possible short range interaction by disorders or spin fluctuation, which is also hinted from the neutron results below. When the magnetic fields were applied along the c axis, the long-range order was suppressed to low temperature and vanished at 0.5 T. Considering the dome shape in the H-T phase diagram in the $NaYbO_2$, we believe this field-dependence relation possibly indicates a different magnetic structure comparing to the up–up–down structure in $NaYbO_2$ [32]. Additionally, a broad peak appears ∼0.15 K at 0.5 T and shifts to higher temperature ∼0.4 K at 0.75 K. This broad peak could be explained by the possible ferromagnetic component and/or Schottky effect.

B. Neutron Scattering

In order to investigate the nature of the long-range magnetic order, as indicated by the heat capacity measurements, neutron powder diffraction patterns were collected between 2 K and 0.08 K. A representative pattern collected above the signal seen in heat capacity (i.e. at 800 mK) is shown together with a best fit model determined by Rietveld refinement (Fig. 2(a).) As seen, the previously reported delafossite crystal structure with $R\bar{3}m$ space group symmetry adequately accounts for the observed peak positions and intensities [40, 42]. Table I lists the crystallographic parameters for two selected temperatures obtained from Rietveld refinements.

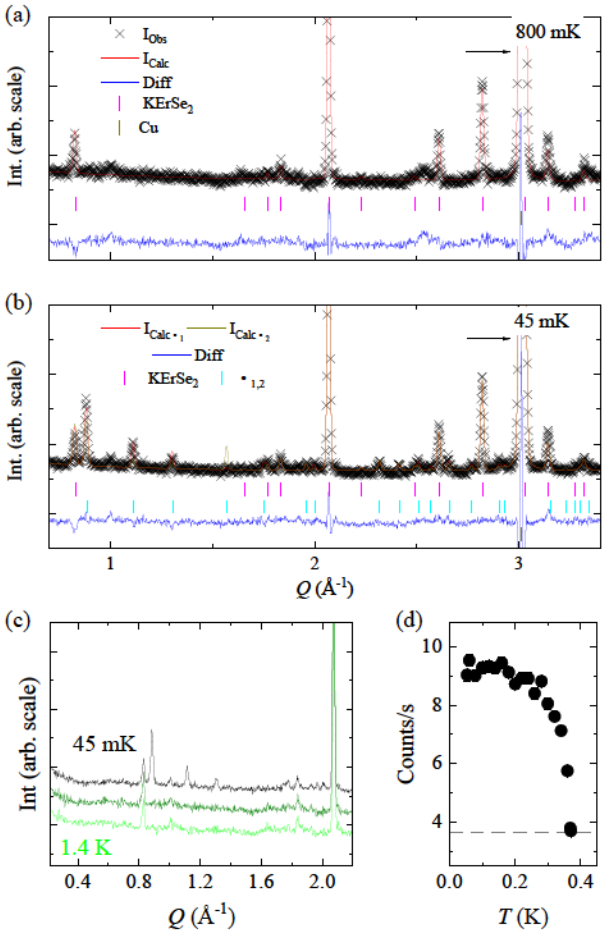

FIG. 2. Neutron powder diffraction data, together with best fit models determined from Rietveld refinements for data collected at (a) 800 mK and (b) 45 mK. In both panels the data, model, difference, and phase peak indexes are indicated by black '×', red lines, blue lines, and magenta '|'tick marks respectively. Indicated by dark yellow tick marks and asterisks are peaks belonging to the Cu sample can. In (b) the cyan tick marks indicate peaks belonging to the magnetic phase generated by the Γ_1 irreducible representation. (c) Neutron diffraction patterns collected at 1.4 K, 800 and 45 mK showing the appearance of new peaks below the transition temperature. (d) Temperature dependence of the $(\frac{1}{2}, 0, \frac{1}{2})$ peak intensity. In (b) the grey line indicates the background intensity for the Q position of the $(\frac{1}{2}, 0, \frac{1}{2})$ peak determined from the 1.4 K diffraction pattern.

Figure 2 (c) shows neutron diffraction patterns collected at 1.4 K and 45 mK, which are above and below the feature temperature of the heat capacity result. As seen, at several positions new peaks arise in the 45 mK data

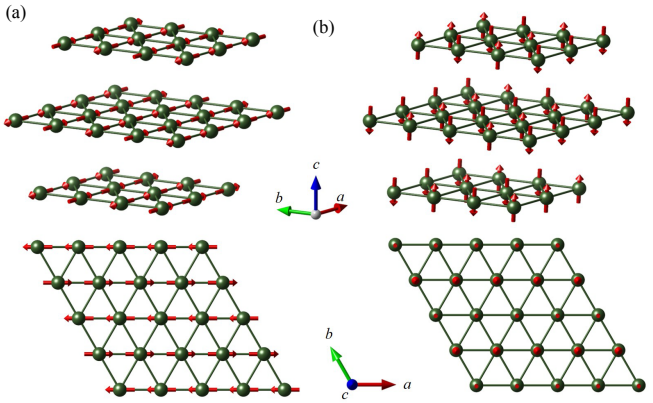

Γ_1 C_c2/m Γ_2 C_c2/c

may be integrated into the diffraction pattern due to the finite energy of the incident neutrons and the diffractometer's inability to discriminate for purely elastic scattering. Looking at the background in Fig. 2, we note that unlike the usually, flat isotropic background observed on the HB-2A diffractometer [43], we see a generally 'lumpy' nonlinear background in both the 800 and 45 mK scans. Such a signal may be indicative of diffuse scattering coming from the sample.

In order to identify any contribution to the background arising from magnetic scattering from the sample we look at difference curves between the sample under different field and temperature conditions as shown in Fig. 4(a). Comparing first the 1.4 K and 45 mK data, we see a slight increase in the background at low Q in the 1.4 K run as might be expected from the paramagnetic state where increased low Q scattering is expected from the bare form factor of the Er^{3+} ion (see for instance 48 or 49). The lack of a significant feature here is consistent with the similarly 'lumpy' background seen in both high and low temperature scans in Fig. 2 which indicates its source persists to 1.4 K.

As another test, we compare low temperature patterns collected in 0 and 4 T applied fields (Fig. 4(a)). In this difference curve a more significant change is apparent, and an obvious dip around 1 $Å^{-1}$ is seen. As will be discussed later, both scans are in a magnetically ordered state and at the same temperature, therefore this cannot be due to paramagnetic scattering from Er^{3+} ions. Instead, this is consistent with the applied field either polarizing static magnetically disordered regions into a FM state, or similarly, pushing fluctuating spins into long-lived (FM) states which contribute to Bragg reflections rather than diffuse scattering [50]. Either of these explanations is consistent with the loss of diffuse intensity around 1 $Å^{-1}$ upon applying a magnetic field. We note that similar difference curves are seen for all applied fields – even the $(45\ mK\ 0.25\ T) - (45\ mK\ 0\ T)$ difference curve exhibits a decreased low q background relative to the zero-field difference curve.

From this observation we suggest it is likely that the reduced ordered moment for Er^{3+} obtained from our Rietveld analysis is due to either partial static disorder where portions of the Er sub-lattice do not conform to the long range magnetic order, or to part of the Er^{3+} ion's unpaired electrons remaining in a fluctuating state (see for instance work on $Er_2Ti_2O_7$ in [51–53]). While our current analysis is insufficient to discriminate between these scenarios decisively, we note that as only a small applied field is able to suppress the diffuse scattering the fluctuation scenario may be more likely as a larger field would be expected necessary to polarize static magnetic disorder. For instance with a Curie-Weiss temperature of $|\theta_{CW}| \sim 4\ K$ we can estimate an overall exchange constant of around 50 meV, considering that the smallest measured field of 0.25 T was adequate to reduce the diffuse background we can estimate an energy scale of $\sim 40\ meV$ to polarize the disordered state. Though both of these

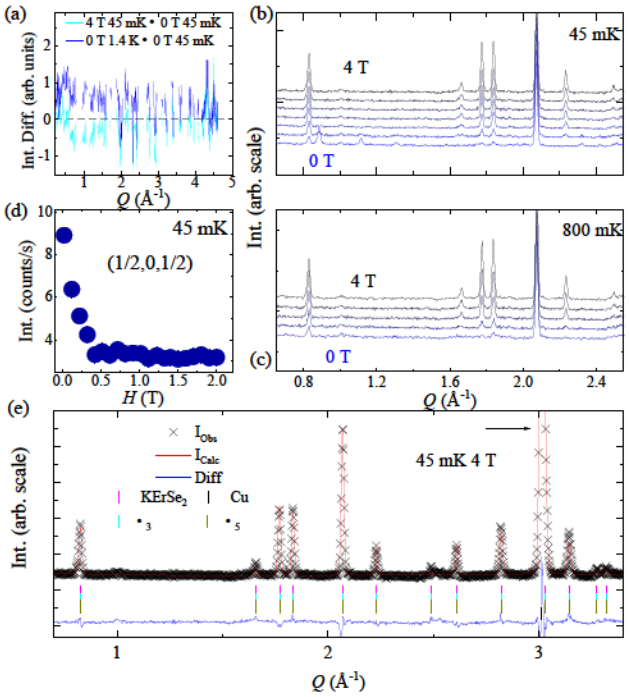

FIG. 4. (a) Difference curves of diffraction patterns collected at various temperatures and fields. Diffraction patterns collected under applied fields at (b) 45 mK and (c) 800 mK. (d) Order parameter scan on the $(\frac{1}{2}, 0, \frac{1}{2})$ magnetic Bragg reflection as a function of applied magnetic field collected at 45 mK. (e) Neutron powder diffraction data, together with best fit models determined from Rietveld refinements for data collected at 45 mK under an applied field of 4 T. The data, model, difference, and phase peak indexes are indicated by black '×', red lines, blue lines, and '|' tick marks respectively. The Cu peaks are also indicated by an arrow due to the overlapping difference curve.

values are rough estimates, they suggest that a larger field should be necessary to overcome exchange interactions. This is corroborated, at least in part, by recent studies explicating the magnetic Hamiltonian which suggested the possibility of quantum fluctuations in the magnetic ground state [42]. However, additional studies on single crystals are needed to look for firmer evidence of diffuse scattering and its potential features in un-collapsed HKL space as well as measuring the spin-waves in the ordered state.

Encouraged by our heat capacity results, we performed neutron powder diffraction measurements under applied magnetic fields to look for a change in the long-range magnetic order. Powder patterns collected at 45 mK and 800 mK under applied fields from 0 to 4 T are shown as waterfall plots in Fig. 4 (b) and (c). At 45 mK, we observe the relatively quick suppression of the $(\frac{1}{2}, 0, \frac{1}{2})$ type magnetic state, with the associated magnetic Bragg peaks disappearing above 0.25 T. On the other hand, while peaks associated with the $(\frac{1}{2}, 0, \frac{1}{2})$ order are suppressed, a significant increase in intensity is seen on several low Q

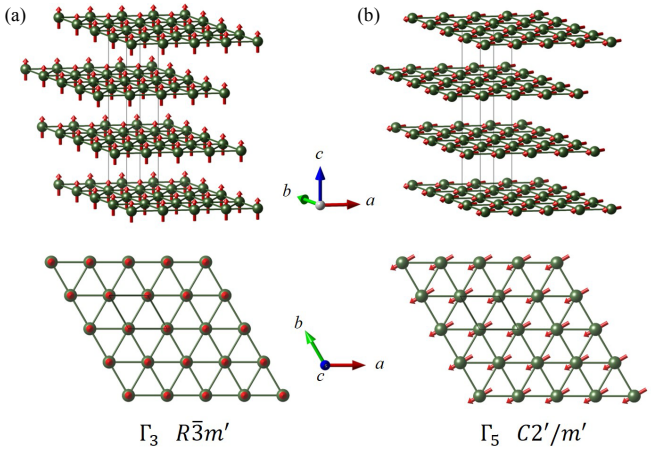

Γ_3 $R\bar{3}m'$ Γ_5 $C2'/m'$

C. Theory Model

$$\sum \qquad \sum$$

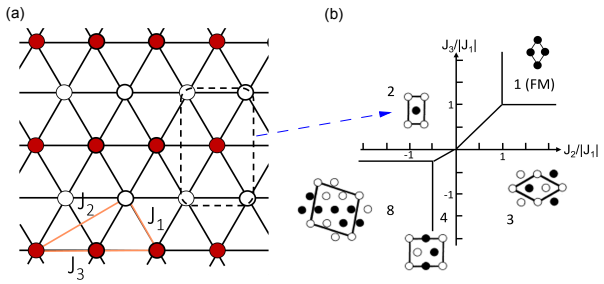

Q

b — –

b — –

Q **b** **b**

IV. CONCLUSION

ACKNOWLEDGMENTS

118

59

8

21

9

464

119

5

120

8

115

60

117

2

4

540

12

13

97

8

81

2

101

67

276

35 **3**

98

89

99

192

27

276-278

100 **44**

100 **3**

8 **101**

58

112

9

101

64

86